

Effect of Long-range Transport from Changing Emission on Ozone-NO_x-VOC Sensitivity: Implication of Control Strategy to Improve Ozone

Tu-Fu Chen¹, Chang-You Tsai², Chien-Hung Chen², and Ken-Hui Chang^{3*}

ABSTRACT

Many efforts on O₃-NO_x-VOC sensitivity have been made to improve O₃ pollution. However, the role of NO_x, VOCs and O₃ itself as well as the sensitivity of O₃ during long-range transport still remains unclear. Therefore, the major aim of this study was to analyze the effect of long-range transport in Northeast Asia (including the countries of China, Korea and Japan) on the O₃ level in Taiwan and subsequently formulate the control strategy to better reduce O₃ levels. A photochemical air quality model was employed in this study to conduct long term simulation in February, May, August, and October during the year of 2007 as the base year. To that end, a previously developed transition indicator was used to determine whether VOCs or NO_x is limited on ozone formation.

The results indicate that with the increase in the emissions of air pollutants in Northeast Asia from 2007 to 2020, the ratio of VOC-sensitive regime with O₃ pollution in Taiwan decreases from 72% to 55%. This means that the strategy for controlling the emissions of air pollutants and improving Taiwan O₃ pollution should be gradually adjusted because equal emphasis should be placed on the reduction of NO_x and VOCs even though the reduction of VOC is of high importance as well. In addition, variations in the wind field in different seasons could lead to the importation of polluted air masses of various degrees of aging from northeastern Asia. In this case, the long-range transport effect in the future would result in more seasonal fluctuation of O₃ sensitivity in Taiwan.

Keywords: Ozone improvement, control strategy, Photochemical indicator, air quality modeling.

1. INTRODUCTION

China located in the region of East Asia is regarded as one of the world's fastest developing countries. Satellite instrument measurements have been used to retrieve tropospheric columns of NO₂ and O₃. Additionally, NO₂ column concentrations near Beijing and Tianjin in China, the Yangtze River Delta, and the Pearl River Delta are significantly higher than those detected in other regions, and every year (Richter *et al.* 2005; Tanimoto 2009; Wang *et al.* 2009). Signs of an increase in O₃ column concentrations detected in the Yangtze River Delta for the long term trend has also been observed. (Xu *et al.* 2006).

It is evident that the serious air concentrations in China have been considered as a result of the influence on the surrounding regions and countries. Nagashima *et al.* (2010) employed a global chemical model of the troposphere to simulate the ground O₃

levels in East Asia from 2000 to 2005. The results indicate that in the springtime in Japan and Korea, only 20 % of the ground O₃ was from local contributions. As noted by Chou *et al.* (2006), the increase in O₃ concentration efflux from the Asia mainland in the past decade has completely offset the reduced O₃ precursor levels in Taiwan through long-range transport (LRT). For this reason, the average O₃ concentration level in Taipei has been increasing the past two decades. Owing to various meteorological parameters across different seasons, the impact of the LRT from East Asia is more significant during winter time in Taiwan. Chou *et al.* (2006) have maintained that the average increase in O₃ transported from China over the past 10 years has offset the improvement in O₃ levels resulting from the emission reduction of O₃ precursors in Taiwan.

Taiwan is considered one of China's neighboring countries. The Influence of air quality as a result of transboundary LRT varies according to different weather conditions throughout the year. Wang (2005) used a Lagrangian model to calculate the airstreams influencing Taiwan between 1994 and 2002. The results showed that the airstream influencing Taiwan is the most stable in summer, with 56 to 67 % of the airstreams coming from the southwest, followed by winter airstreams, with 48 to 58 % coming from the northeast and 39 to 44 % from the north. Airstreams in spring may come from anywhere in East Asia. This indicates that both the path and the level of influence of LRT on Taiwan would differ according to seasons. With a gradual increase in the emission levels observed from neighboring countries, the influence of LRT may even exacerbate O₃ pollution in Taiwan. Ac-

Manuscript received July 15, 2021; revised August 24, 2021; accepted September 7, 2021.

¹ Assistant Researcher, Department of Safety, Health and Environmental Engineering, National Yunlin University of Science and Technology, Taiwan 64002, R.O.C.

² Ph.D. Student, Department of Safety, Health and Environmental Engineering, National Yunlin University of Science and Technology, Taiwan 64002, R.O.C.

^{3*} Professor (corresponding author), Department of Safety, Health and Environmental Engineering, National Yunlin University of Science and Technology, Taiwan 64002, R.O.C. (e-mail: changken@yuntech.edu.tw).

ording to estimates from the Regional Emission Inventory in Asia (REAS) (Ohara *et al.* 2007), the total emissions from East Asia of NO_x and NMHC is at 31 and 52 million tons, respectively. This will approximately increase to 46 and 84 million tons by 2020 (the most significant growth scenario reported in that study, Policy Failed Case (PFC) 2020).

Tropospheric O₃ is a secondary pollutant generated by the photochemical reactions of atmospheric NO_x and VOCs. If the O₃ can be effectively reduced through the control of the NO_x emission, the phenomenon is thus called a NO_x-sensitive regime (NSR). Alternatively, if the O₃ level can be decreased by controlling the VOCs, it is referred to as a VOC-sensitive regime (VSR). The sensitivity of O₃ to the precursors is called O₃ sensitivity. The development of the various photochemical indicators can assess O₃ sensitivity with the direct comparison between the indicator transition value and field observations (Sillman and He 2002). The indicator transition value is an interval with an upper and a lower limit. Take H₂O₂/HNO₃ for example (Chen and Chang 2006), if the indicator value is greater than the upper limit, the observed location is of NSR; if the observation value is smaller than the lower limit, the observed region is of VSR. Also an observation value between the upper and lower limits indicates that the influence of NO_x and VOC emission-reduction on O₃ levels are comparable, and so this is called a transition regime (TRR).

Sillman *et al.* (1997) initially proposed that the transition value of a good indicator should remain constant in different simulations. Because the studies into indicator transition values evolve over time, some researchers believe that the indicator transition value changes with environmental conditions (*e.g.* Lu and Chang 1998; Chock *et al.* 1999) and that this is systematically related to the degree of pollution (Tonnesen and Dennis, 2000; Sillman and He 2002). Later, Chen and Chang (2006) found that the indicator transition value changes with grid locations and meteorological parameters, and that change in the grid indicator transition value can be illustrated by an equation comprised of peak O₃, NO_z, and H₂O₂/HNO₃. This is called the indicator transition value equation for air mass (ITVEAM).

Additionally, according to an estimate reported by the REAS (Ohara *et al.* 2007), human emissions of NO_x and VOCs in Northeast Asia will have increased by approximately 48 and 62%, respectively, by 2020, in comparison with the emissions detected during the year of 2007. Clearly, with the gradual increase of emissions from neighboring countries in the future, the effect of LRT may further exacerbate the problem of O₃ pollution in Taiwan. The effects of LRT on O₃ in Taiwan would directly increase not only O₃ concentrations but also NO_x and VOCs. This might in turn lead to the indirect formation of O₃ in Taiwan.

To date, most of the previous studies that used the three-dimensional Eulerian air quality model for the investigation of LRT were conducted with only short term episodic simulations, and the discussion was limited to the effect of LRT on O₃ concentrations. Although many local studies have been conducted to look into whether the formation of O₃ is NO_x or VOC limited, and so appropriate control strategy can be formulated (He *et al.* 2017; Jin *et al.* 2017; Inoue *et al.* 019), very little attention has been paid to the transboundary studies of O₃ to further determine whether the local region is VSR or NSR. Consequently, the present study was undertaken to model the effect of LRT on O₃ levels in Taiwan and so to determine the effect as such on any changes of whether VOC or NO_x is limited in Taiwan, and so the authorities can formulate suitable strategies for local emission control. In particular, using ITVEAM in conjunction with daily

frequency exceeding 1-h peak O₃ 120 ppb, the resultant grid cell land (in km² d) affected by future transboundary emissions obtained from LRT can be quantified.

2. METHODS

2.1 Air quality model system

This study used Taiwan Air Quality Model (TAQM) for the long term simulation of three levels of nested domains (Fig. 1). Domain 1 mainly encompasses the regions of Northeast Asia (81 × 81 km²); Domain 2 encompasses particularly the southeastern provinces of China and Taiwan (27 × 27 km²); and Domain 3 encompasses the entire Taiwan with higher resolution grid cells (9 × 9 km²). TAQM was initially developed and based on the Regional Acid Deposition Model ver. 2 (Chang *et al.* 1987; Chang 1990) for simulating the air quality of East Asia. TAQM considers different processes of atmospheric advection, diffusion, chemical reaction, cloud effect, dry/wet depositions, and source emission (Chang *et al.* 2000), and uses the simulation data of Mesoscale Model ver. 5 (Grell *et al.* 1993) as the meteorological inputs for the model. The simulation periods of the model were February, May, August, and October of 2007, with each month representing the winter, spring, summer, and fall seasons, respectively; therefore, the results obtained during these four months with the long term simulation could represent the conditions for the base year of 2007.

The 2020 simulations were performed for investigating the effects of emission growth in Northeast Asia on the O₃ levels in Taiwan. The emission data in Taiwan at high resolution (1 km × 1 km) were used for the base year of 2007, and the emission data of other northeastern Asian regions were at relatively lower resolution (0.5° × 0.5°). TEDS7 (Taiwan EPA, 2009) was adopted for anthropogenic emissions in Taiwan, and the Taiwan Biogenic Emission Inventory System (TBEIS) was utilised in coordination with meteorological data for the estimation of hourly biogenic emissions (Chang *et al.* 2009). The REAS estimation data (Ohara *et al.* 2007)

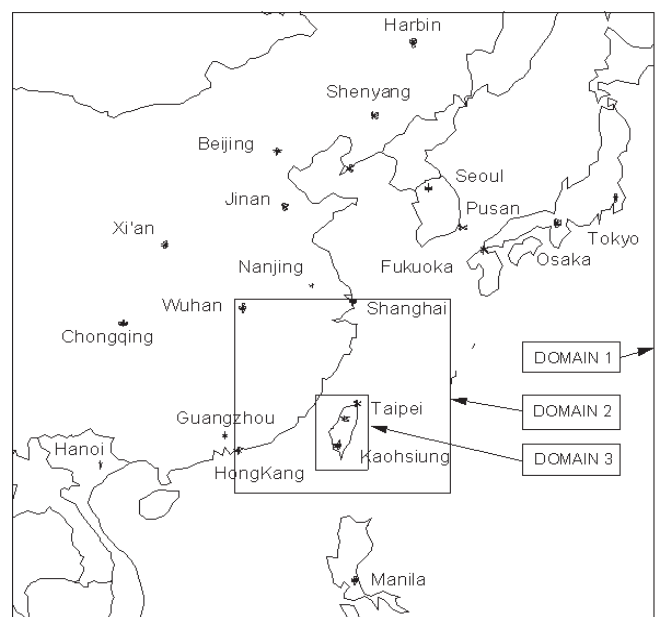


Fig. 1 Configuration of three-level nesting domains in the TAQM.

were considered for anthropogenic emissions in the regions of East Asian. The East Asian Biogenic Emission Inventory System (EABEIS) (Chen *et al.* 2020) was adopted in coordination with meteorological data for the estimation of hourly biogenic emissions. For the emissions detected in the year of 2020 in Taiwan, the level was the same as that observed in the year of 2007 without any increase. The only difference between the emissions for the 2020 case and the Base case is that for the former, the most significant case of the growth of anthropogenic emissions (PFC2020) in East Asia, as estimated by the REAS (Ohara *et al.* 2007), was the anthropogenic emissions detected in other East Asia regions while the data for the meteorological parameters, biogenic emissions, and anthropogenic emissions in Taiwan were the same when both of the cases were considered.

2.2 Simulation period and cases

Four months including February, May, August, and October were selected for simulations to represent as winter, spring, summer, and autumn. The combined results of the long-term simulation during these 4 months were found to be representative of those observed in the year of 2007.

Three cases of emission setup were simulated to uncover the influence of the growth of the emissions detected in the East Asian region emissions on the concentrations of O₃ in Taiwan. A base case and two control cases were included in these simulations. All sources emitted from all the countries and areas in East Asia in the year of 2007 were considered in the Base case. Case 1 only was undertaken to look into the sources emitted across Taiwan (ignoring the sources outside of Taiwan) in year 2007. Case 2 was performed to consider all sources emitted from all of the areas in East Asia in year the year of 2020. The difference between the Base case and Case 1 (Scenario 1) was the influence on Taiwan mainly resulted from LRT in the base year of 2007. The difference between Case 2 and Case 1 (Scenario 2) was the influence on Taiwan from LRT in the year of 2020. The difference between the Base case and Case 2 (Scenario 3) was the influence of the additional LRT on Taiwan in the future from 2007 to 2020.

2.3 Analyzing the influence on O₃ concentrations

To better quantify the influence from LRT, the daily average maximum concentrations of O₃ (MADMO₃) per month in each simulation case was calculated. By comparing the O₃ simulation results of different cases, we could clarify the contribution of LRT to the MADMO₃ concentrations. That was because the influence from LRT may cause the hourly concentration level of O₃ to get lower in some areas of Taiwan than the value required for the classification of the polluted O₃ (above 120 ppb). Thus, in this study, the area polluted by O₃ was also considered as a quantitative measure to be combined with the influence of LRT. To that end, O₃ pollution areas were quantified, using the grids (9 km × 9 km), with the peak O₃ concentrations higher than 120 ppb polluted. To obtain the results, the number of grids multiplied against the days with peak O₃ concentrations above 120 ppb and the grid area was summed up. Also, it was assumed that more than one occurrence of O₃ pollution in the same grid detected in a single day was considered a form of pollution.

3. RESULTS AND DISCUSSION

3.1 Meteorological condition analysis

Fig. 2 depicts the ground flow fields from the National Centers

for Environmental Prediction (NCEP). The vertical flow field graphs at a latitude of 23.5°N is the latitudinal line passing through Taiwan. Winter is from December to February in Taiwan. In February, the weather of Taiwan in winter is most influenced by the northeast monsoon. The ground flow field indicates that the area around Taiwan was primarily dominated by a northeasterly wind because Taiwan is located downwind of the East Asia pollution flow efflux. The vertical flow field shows that the pollutants from China may creeping into Taiwan through the 750 to 850 hPa air stream.

Spring in Taiwan runs from March to May. During May, the flow field surrounding Taiwan gradually shifts from northeasterly flow to southwesterly flow. Thus, the airstream is comparatively turbulent. The ground flow graph shows that a low pressure circular flow field existed on the sea to the northwest of Taiwan. The eastern part of Taiwan was significantly influenced by an easterly wind airstream system, while, in contrast, the wind field on the western side of Taiwan was turbulent because of the lee vortex effect. Additionally, the lower wind speed was not conducive to the dispersal and dilution of pollutants. Combined with the vertical flow field structure, at this time, the flow field would be conducive to pollutant transport from China to Taiwan.

In Taiwan, summer is from June to August. In August, the southwesterly wind is the prevailing wind in Taiwan. The flow field graph shows that the wind system around Taiwan was mainly southerly, with a relatively clean airstream from the ocean. The vertical circulation flow shows large areas of downdraft with less eastern-western horizontal flow, which further isolates the transport of pollutants from China to Taiwan.

Besides, autumn runs from September to November. In October, the northeasterly seasonal wind begins to influence Taiwan. This is mainly attributed from the high air pressure system set in Mongolia, China, Siberia, and the northeastern Asian area around Japan. The ground flow field indicates that Taiwan and surrounding areas were dominated by the northeasterly wind. This means that Taiwan was located downwind of the East Asian pollutant efflux. The vertical flow field shows that pollutants from China may be pouring into Taiwan through an airstream ranging between 450 and 750 hPa.

3.2 Simulation Verification

To verify the accuracy of the model, the three monitoring stations outside Taiwan chosen as the sites are the islands of Kinmen, Matsu and Japan-Yonguniima. Also, three background air ambient monitoring stations on Taiwan island (Wanli, Hengchun, Taitung) were selected. The location of each station is illustrated in Fig. 3.

Fig. 4 shows the hourly comparisons of the simulated and observed O₃ values in October. The daily and nightly changes in O₃ levels were consistent with those observed at the Wan-Li, Heng-Chun, and Tai-Tung stations in Taiwan, except for the fact that the simulated values were significantly higher than those observed at the beginning of the simulations. This phenomenon might have been due to the hypothesized initial and boundary values. Nonetheless, the simulated and the observed values indicate that the estimated emissions in Taiwan were well predicted. The long term trend of the simulated O₃ values at the Kin-Men and Mat-Zu stations, which are closer to China, were similar to the observed ones; but the simulated values of these two stations were incomparable with those values observed on certain dates, particularly between October 7 and October 10. The inconsistency might have been potentially caused by the unstable wind fields because the weather systems were under transition during that period. Another potential factor is that the simulated values of these two stations were obtained from Domain 2.

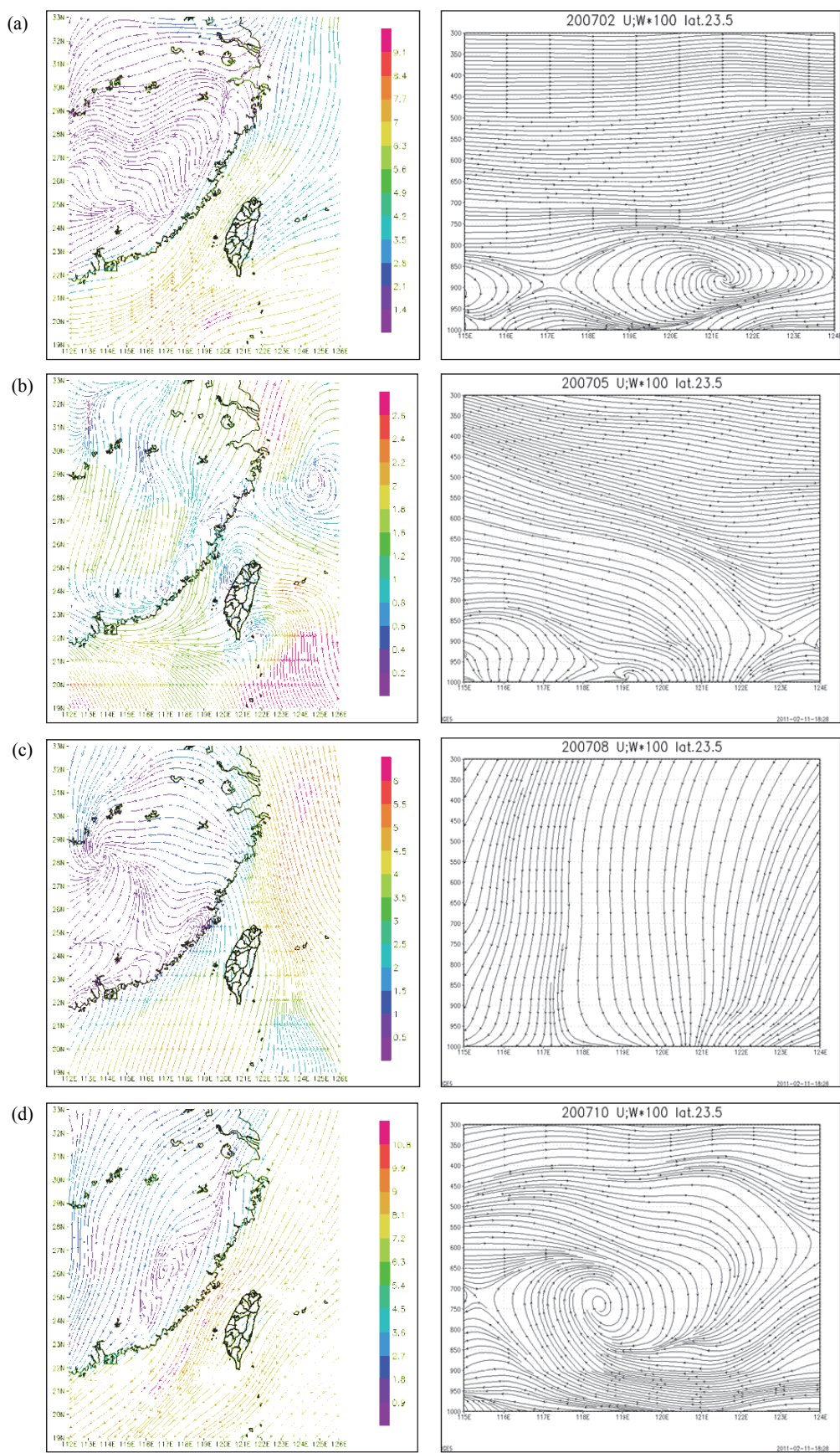


Fig. 2 The NCEP's monthly average ground flow fields (left) and latitudinal vertical flow fields (right) in (a) February, (b) May, (c) August and (d) October.

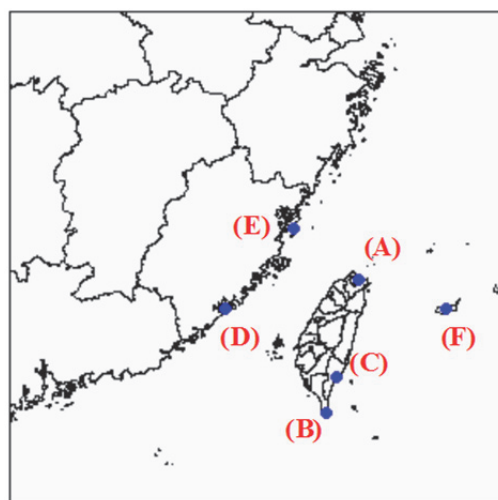


Fig. 3 The locations of monitoring stations in (a) Wanli, (b) Hengchun, (c) Taitung, (d) Kinmen, (e) Matzu, and (f) Japan Yonagunijima.

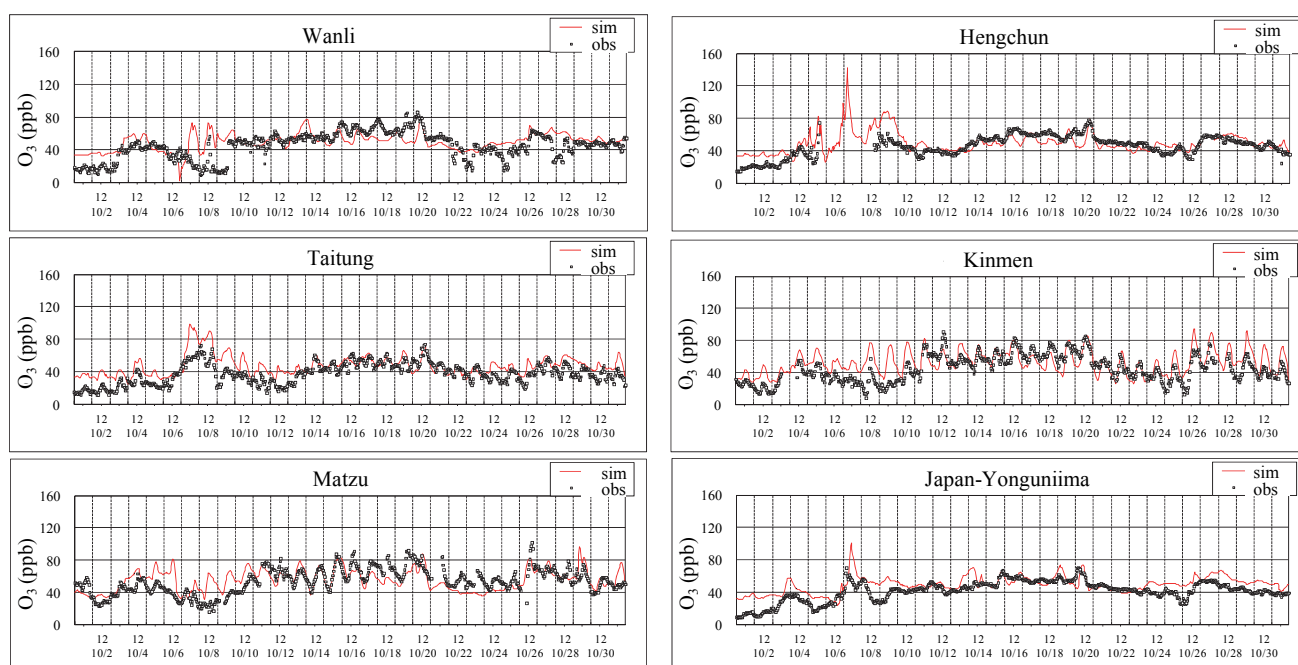


Fig. 4 Temporal comparisons made with the O₃ concentrations at the six monitoring sites selected

Yonagunijima island is a small island located to the east of Taiwan. The island has no apparent source of pollution, and so the cause of the variation in O₃ levels was the transport of pollutants from outside the island. The simulation results at Yonagunijima station were also good, and the overall trend of the simulation was consistent with the observed values. This indicates the meteorological field was managed accurately. Again, the over-estimated simulated values at the beginning of the simulation were also assumed to result from the setting of the initial and boundary values.

The error analysis of the simulated values and observed values during these four months is listed in Table 1. As can be seen clearly from Table 1, the error detected in August was comparatively higher (overall bias = 24%). In contrast, the error

for the other three months was comparatively lower. The major reason for the high error in August would be due to the fact that the southwest monsoon winds blow with the air flow coming from the oceans. As a result, the simulated concentration would be significantly affected by the simulated boundary value setting. Also, when the boundary value is set too high, an overestimation of the simulated concentration would easily occur. Generally, the overall bias was approximately 17% with the gross error 27% at the six stations over the four months, and the long term simulated trend closely followed the observed values. These results suggest that most of the error data occurred within the benchmark range used to evaluate the model performance (Emery *et al.* 2001; Russell and Dennis 2000), and the simulated results would be acceptable for long term simulations.

Table 1 The performance evaluation of O₃ concentration simulation

	Overall bias of hourly O ₃ ^a	Gross error of hourly O ₃ ^b
Feb.	0.13	0.21
May	0.22	0.29
Aug.	0.24	0.40
Oct.	0.10	0.20
Ave.	0.17	0.27

$$^a \text{Overall bias} = \frac{1}{N \times M} \sum_{k=1}^M \sum_{i=1}^N (P_{i,k} - O_{i,k}) / O_{i,k}$$

^b Gross error = $\frac{1}{N \times M} \sum_{k=1}^M \sum_{i=1}^N |P_{i,k} - O_{i,k}| / |O_{i,k}|$, where $P_{i,k}$ is the predicted value at (location, time)_{*i,k*}, $O_{i,k}$ is the observed value at (location, time)_{*i,k*}, M is the total number of monitoring sites, and N is the total number of pairs.

3.3 Influence of LRT on O₃ concentrations in Taiwan

The MADMO3 concentration from the base cases in each season are provided in Fig. 5. The spatial distribution of the Base case demonstrates that the O₃ concentration on the western part of Taiwan was consistently higher than that in the eastern part of Taiwan. The main reason for this phenomenon was that most of the cities, industrial zones, and the population are concentrated in the western part of Taiwan. Besides, seasonal winds from different directions influence Taiwan during different seasons. This causes the locations with high O₃ concentrations to differ slightly between seasons. The prevailing northeasterly seasonal wind in winter (February) and autumn (October) could make the high-O₃ concentration area denser and so extended the high-O₃ concentration area toward the seas in the southwest. The dominant southwesterly seasonal wind in summer enabled the O₃ concentration area to move to the northern sea surface. Spring season (May) occurred during the transition between northeasterly winds to southwesterly winds. It is therefore clear that areas with high O₃ concentrations are not only concentrated inland but also extended toward the north.

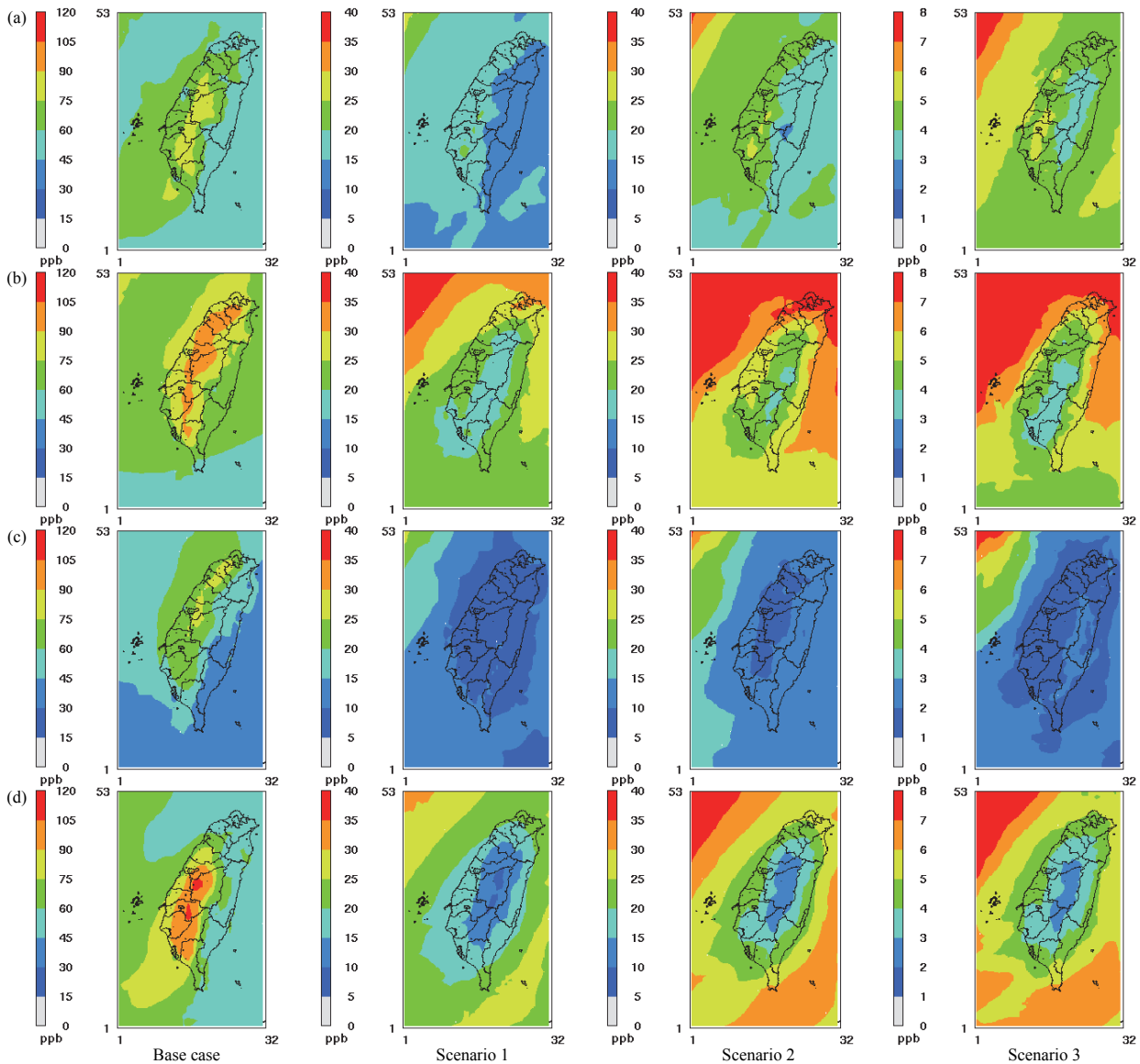


Fig. 5 The influence on the monthly average daily peak ozone concentrations from transboundary long-range transport in (a) February, (b) May, (c) August and (d) October.

The largest influence of LRT in 2007 on Taiwan (Scenario 1) occurred in spring. The most heavily influenced region was the coastal area in the north of Taiwan, with upwards of 30 ppb from transport, diminishing gradually inland. In winter, the western part of Taiwan was influenced more than the east, to the extent of 15 to 20 ppb. In autumn, the coastal areas were the most influenced, to a range of 20 to 25 ppb, diminishing gradually inland. In summer, the airstream from the southern ocean was relatively cleaner and the least affected. However, a trend of decrease from the southern seas to inland could be observed, with small areas under more than 10 ppb of influence. The influence of LRT on Taiwan in 2020 (Scenario 2) was distributed similarly as that in Scenario 1, but with a heavier influence. The largest effect occurred during the spring season, with more than 35 ppb influenced. The additional influence between 2007 and 2020 (Scenario 3) also had a similar spatial distribution as that of Scenario 1 and Scenario 2.

Table 2 shows the MADMO3 concentrations for all the land grids in Taiwan. The total influence during the whole year was represented by the averages of the 4 months. Without emissions from East Asia, the O₃ concentration from Taiwan was only 53.7 ppb. When East Asian emissions were included in the analysis, the O₃ concentration increased to 69.3 ppb. This indicates that LRT accounts for 15.5 ppb of O₃ concentrations in Taiwan, or 22.4 % of the base case. Even if the emissions in Taiwan remain the same, the additional emissions from other East Asian countries would increase the O₃ concentration in Taiwan to 73.0 ppb by 2020, under the worst case scenario. In other words, the O₃ concentration in Taiwan would get worse by 3.7 ppb, or 5.4 % of the base case concentration.

The emission of the O₃ concentration in Taiwan was higher during the seasons of spring (May) and autumn (October) at approximately 58 ppb. The effect of emissions from Taiwan was less during winter (February) and summer (August) at approximately 49 ppb. When the emissions from East Asia were included in the analysis, O₃ concentrations differed significantly between the high and low seasons because of seasonal LRT variations. Spring and autumn still showed the highest concentrations (80.2 and 73.4 ppb, respectively), and winter and summer O₃ levels remained lower (65.1 and 58.0 ppb, respectively). During spring, the ground flow fields, high-altitude flow fields, and vertical flows all demonstrated the possibility for the pollutants from

the continent to travel to Taiwan, and so resulted in the largest contribution of LRT to O₃ concentrations at 22 ppb. The prevailing winds during summer were the relatively clean southerly winds from the southern seas, with a lower influence from LRT of 9 ppb. The northeasterly winds dominated both autumn and winter, and the downwind position from East Asia pollutant efflux created a higher influence than that during summer. The effect of LRT in winter and autumn were similar at approximately 16 ppb. In the worst case scenario in 2020, the summer O₃ concentration increased to 85 ppb. Therefore, if the additional influence in different seasons had been used as criteria, the influence in spring would have been the most serious (4.9 ppb), followed by winter (4.4 ppb), with the least amount of influence expected in summer (1.7 ppb).

3.4 Effect of East Asian Emissions on the O₃ levels in Taiwan

To better represent all the areas affected by O₃ in Taiwan, all land grid cells in Taiwan were included in the statistical analyses. The DMO3 levels of all land grid cells in Taiwan in the Base year and the year of 2020 were averaged, and the differences between the two cases indicated the LRT on future DMO3 in Taiwan. Fig. 6 shows the averaged results of each of the four months.

Using the averaged data of the four months to represent the effect of O₃ emissions for the entire year, the annual average of DMO3 (AADMO3) in Taiwan for the Base case (2007) was 69 ppb. However, even if the emissions in Taiwan remained the same as in 2007, new emissions from other northeastern Asian countries in the future (2020) would elevate the AADMO3 of Taiwan to 73 ppb; the AADMO3 in Taiwan would worsen by 4 ppb. In Taiwan, the lowest was 58 ppb in summer (August), and the effect of the future growth from transboundary emissions was also lowest in summer (an increase of 2 ppb). The highest MADMO3 was 80 ppb in spring (May), and the effect of the future emissions was also the highest in spring (increase by 5 ppb). Additionally, though the MADMO3 (65 ppb) in winter (February) was not as high as that in spring, the effect of the future emissions (an increase of 4 ppb) was only slightly lower than that in spring. It is noted that some of the data are for background values, thus 2-5 ppb increase of MADMO3 is significant.

Table 2 The influence of the East Asian emissions on the monthly average daily peak ozone concentrations for the months of February, May, August, and October, 2007.

	Conc. of MADMO3 ^a			Increased conc. of MADMO3 ^a			Ratio of increased conc. of MADMO3 ^a		
	Base case ^b (ppb) (A)	Case 1 ^c (ppb) (B)	Case 2 ^d (ppb) (C)	Scenario 1 ^e (ppb) (A-B)	Scenario 2 ^f (ppb) (C-B)	Scenario 3 ^g (ppb) (C-A)	Scenario 1 ^e (%) (A-B)/A	Scenario 2 ^f (%) (C-B)/A	Scenario 3 ^g (%) (C-A)/A
February	65.1	49.5	69.5	15.6	20.0	4.4	24.0	30.8	6.8
May	80.2	58.6	85.0	21.6	26.5	4.9	26.9	33.0	6.1
August	58.0	49.1	59.7	8.9	10.7	1.7	15.4	18.4	3.0
October	73.4	57.3	77.3	16.1	20.0	3.9	21.9	27.2	5.3
Average	69.3	53.7	73.0	15.5	19.3	3.7	22.4	27.8	5.4

a. MADMO3: Monthly average daily maximum ozone

b. Base case: emissions including all countries and areas in the year of 2007.

c. Case 1: emissions including all countries and area except for Taiwan.

d. Case 2: emissions including all countries and areas in the year of 2020.

e. Scenario 1: the LRT effect on Taiwan O₃ for the year 2007.

f. Scenario 2: the LRT effect on Taiwan O₃ for the year 2020.

g. Scenario 3: the LRT effect on Taiwan O₃ between the years of 2007 and 2020.

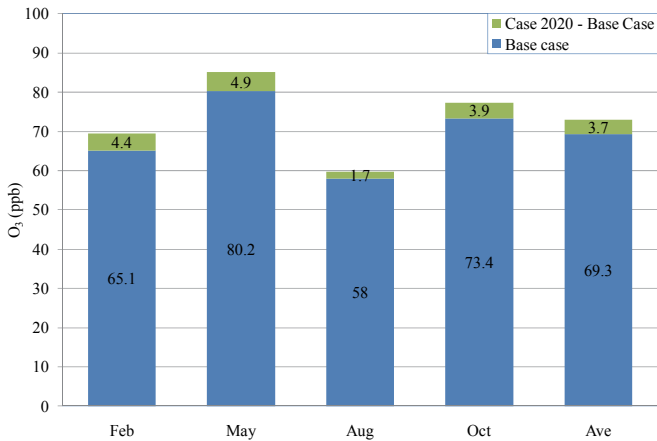


Fig. 6 The effect of the growth in the East Asian emissions on the DMO3 in Taiwan from 2007 to 2020 (the average value of each month)

3.5 Effect of LRT on the Direction of O₃ Pollutant Control in Taiwan

The aim of this study was to understand which precursors would be the most effective ones to the reduction of O₃ pollution. According to Taiwan EPA air quality standards, DMO3 ≥ 120 ppb is regarded as poor air quality. Therefore, when using the ITVEAM proposed by Chen and Chang (2006) for conducting O₃ sensitivity analysis, we specifically focused on the land grid cells with DMO3 ≥ 120 ppb (called O₃-polluted grid cell below) and 120 > DMO3 ≥ 100 ppb. The main reason for the focus placed on the grid cells of 120 > DMO3 ≥ 100 ppb was that grid cells lower than 120 ppb in the Base year may exceed 120 ppb in Case 2020.

Figs. 7 and 8 describe the analytical results of O₃ sensitivity of all O₃-polluted grid cells in the Base year and the year of 2020, respectively. The number beneath each plot is the accumulated grid-cell area (km² d) associated with VSR, NSR, and TRR. The accumulated grid-cell area was obtained by the multiplication product of the number of days, especially for those days when the Taiwanese land grid cells exceeded a DMO3 of 120 ppb within the grid-cell area (9 × 9 km²). Therefore, the seasonal accumulated area would be only accumulated during one month while, in contrast, the annual accumulated area would be accumulated during these four months.

As clearly shown in Fig. 7, the annual result for the Base year indicates that the ratio of VSR was relatively high (72%). Also, TRR was as high as 17%, and NSR was only 11%. Additionally, the ratio of VSR was also the highest in comparison with all of the seasons. The VSR was the highest in winter (85%) with the absence of the NSR grid cell. Even in fall, when VSR was lowest (61%), the ratio was as high as 20% with TRR. This result indicates that controlling VOC emissions should be a priority for Taiwan in effectively reducing the high levels of O₃ pollution.

The pattern for O₃ sensitivity was completely different with future trans-boundary emissions. Clearly, as shown in Figs. 7 and 8, for the purpose of comparison, the area shifted from VSR to NSR. For example, although the annual result for 2020 indicates that the ratio of VSR declined from 72% to 55%, the ratio was still as high as 26% with TRR, and NSR increased to 19%. As for the seasonal results, the VSR ratio all decreased while both the

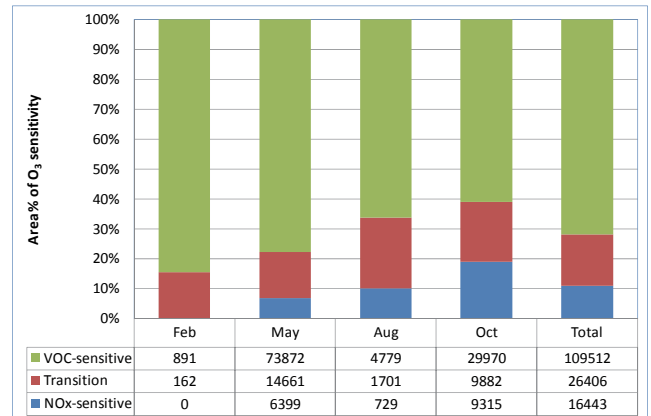


Fig. 7 The analytical results for the O₃ sensitivity of the grid cells polluted with ozone of in the Base case for each month, and the accumulated area and the ratios of VSR, NSR, and TRR; area unit: km²-d

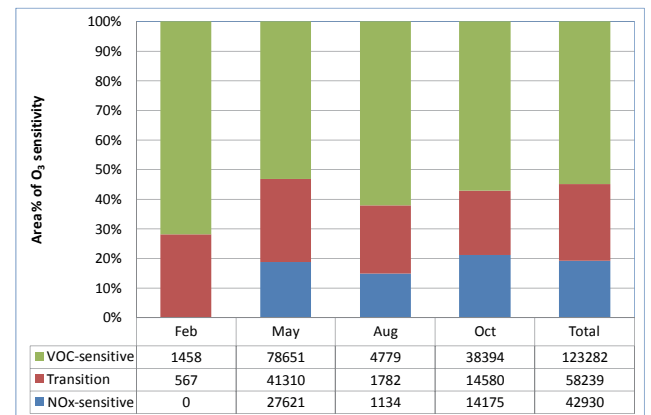


Fig. 8 The analytical results for the O₃ sensitivity of the grid cells polluted with ozone in Case 2020 for each month, and the accumulated area and the ratios of VSR, NSR, and TRR; area unit: km²-d

TRR and NSR ratios increased. The ratio change was the most obvious in spring, as the ratio of TRR and NSR increased from 23% to 47%. As a result, these results indicate that controlling VOC emissions should still be a priority for Taiwan in effectively reducing high levels of O₃ pollution, and yet the increasing importance of NSR should also be recognized.

Though Case 2020 showed increases in the NSR and TRR ratios and a decrease in the VSR ratio in relation to the Base 2007 year, the areas of NSR, TRR, and VSR all increased. The only notable difference is that the increases of NSR and TRR were more apparent than that of VSR because the area polluted by O₃ in Taiwan would increase by 72090 km² d, and of which, 37% would be NSR, and 19% would be VSR. The O₃-polluted area in summer was the smallest (486 km² d), and most of the area (83%) was NSR, but VSR. Although the increase in O₃-polluted area was also small in winter (972 km²-d), most of the area (58%) was VSR without NSR. The O₃-polluted area was greater in spring and fall (52650 km²-d and 17982 km²-d, respectively); although the NSR and VSR patterns were not as extreme as those in summer and winter, NSR was approximately 40% of the increased area and was greater than that of VSR (9%) in spring. However, the phenomenon was the opposite in fall (27% for NSR and 47% for VSR).

The extreme difference between summer and winter was due to the occurrence of the northeastern monsoon, with its high wind speed, in winter in Taiwan. Pollutants are directly imported to Taiwan, and the polluted air mass is relatively fresh; therefore, NSR was absent in the increased area. In summer, Taiwan has a southwestern monsoon; the upwind comes in from the oceans, and thus the imported air flow is usually relatively clean. Even if a polluted air mass is imported, the air mass would be aged; and thus almost all of the increased area was NSR, absent VSR. In spring, the air flow in Taiwan transforms from northeastern to southwestern monsoons, and the air flow is turbulent and slow. This results in lower ground wind speed and slower transport of pollutants. For this reason, NSR was greater than VSR in the increased area. In fall, the northeast monsoon begins to affect Taiwan; and because the wind velocity is high, the air mass imported to Taiwan is relatively fresh. However, the vertical flow field indicates that pollutants from China was possibly imported to Taiwan via an air flow of 450 to 700 hPa. Consequently, this indicates that this part of the air mass is comparatively aged and that both the VSR and NSR would possess a substantial ratio in the increased area.

Thus far, this section has discussed the overall differences in O₃ sensitivity between the Base case and Case 2020. However, the transition of O₃ sensitivity in grid cells caused by the increased long-range transport (that is, Case 2020 - Base case) could not be identified. This transition was classified into the following three main types: unchanged control direction, movement toward VSR, e.g., the transition of NSR into VSR, NSR into TRR, and TRR into VSR and movement toward NSR, e.g.,

includes the transition of VSR into NSR, TRR into NSR, and VSR into TRR, as provided in Table 2.

Table 4 clearly shows how the growth of emissions detected in East Asia from the year of 2007 to the year of 2020 would change the O₃ sensitivity of areas highly polluted with O₃ in Taiwan. The annual data indicates that the ratio of unchanged directions on areas polluted by O₃ was relatively large (82%); whereas the area of transition toward NSR (15%) was significantly greater than the areas of transition toward VSR (3%). From the perspective of seasonal results, the ratio of unchanged control direction was relatively large (72 to 97%) on the areas polluted by O₃ in each season. The area of transition toward NSR was greater than the area of transition toward VSR in spring, summer, and fall; whereas the situation was the opposite in winter. These results indicate that the air mass imported in Taiwan in winter would be relatively fresh, whereas the air masses imported in spring, summer, and fall would be relatively aged. Thus, the annual results show that the growth in East Asian emissions would bring aged air masses and so push the O₃ sensitivity in Taiwan to move toward NSR. Additionally, the areas of direct transition from NSR to VSR or direct transitions from VSR to NSR were small, as given in Table 4. This result is in line with the general fact that the addition or elimination of considerably high concentrations of NO_x or VOCs is required if to cause a dramatic change in O₃ sensitivity is a priority in this regard. Therefore, this part of the results indicate that a direct transition between NSR and VSR is not easily done through LRT in Taiwan and so most of the transitions are between NSR or VSR and TRR.

Table 3 Effects of the East Asian emissions on the ozone pollution area for the months of February, May, August, and October, for the year 2007, in Taiwan.

	Polluted area			Polluted area increased			Ratio of polluted area increased		
	Base case (km ² -d) (A)	Case 1 (km ² -d) (B)	Case 2 (km ² -d) (C)	Scenario 1 (km ² -d) (A-B)	Scenario 2 (km ² -d) (C-B)	Scenario 3 (km ² -d) (C-A)	Scenario 1 (%) (A-B)/A	Scenario 2 (%) (C-B)/A	Scenario 3 (%) (C-A)/A
February	1053	243	2025	810	1782	972	76.9	169.2	92.3
May	94932	14175	147582	80757	133407	52650	85.1	140.5	55.5
August	7209	3159	7695	4050	4536	486	56.2	62.9	6.7
October	49167	25191	67149	23976	41958	17982	48.8	85.3	36.6
Average	152361	42768	224451	109593	181683	72090	71.9	119.2	47.3

Table 4 The effect of the growth in the East Asian emissions from 2007 to 2020 on the O₃ sensitivity of the grid cells polluted in Taiwan by O₃

		February			May			August			October			The Sum of the four months		
		Polluted Area (km ² -d)	Total (km ²)	(%)	Polluted area (km ² -d)	Total (km ²)	(%)	Polluted area (km ² -d)	Total (km ²)	(%)	Polluted Area (km ² -d)	Total (km ²)	(%)	Polluted Area (km ² -d)	Total (km ²)	(%)
Tends Toward VSR	NSR→VSR	81			81			0			162			324		
	NSR→TRR	162	405	20	1296	2592	2	0	0	0	1134	3321	5	2592	6318	3
	TRR→VSR	162			1215			0			2025			3402		
Control Direction unchanged	VSR→VSR	1215			77355			4779			36207			119556		
	TRR→TRR	243	1458	72	23814	118827	81	1620	7452	97	9315	57186	85	34992	184923	82
	NSR→NSR	0			17658			1053			11664			30375		
Tends Toward NSR	VSR→TRR	162			16200			162			4131			20655		
	TRR→NSR	0	162	8	9882	26163	18	81	243	3	2511	6642	10	12474	33210	15
	VSR→NSR	0			81			0			0			81		
Total		2025			147582			7695			67149			224451		

^a NSR: NO_x-sensitive regime ^b VSR: VOC-sensitive regime ^c TRR: transition regime

4. CONCLUSIONS

In this study, the long term air quality simulation models were used during the four months (February, May, August, and October) to represent winter, spring, summer, and fall. The results derived from these four months were considered to represent the conditions of the whole year. The contribution of LRT to the MADMO₃ concentrations in the year of 2007 was approximately 15.5 ppb. To better illustrate this, Assuming the emissions from Taiwan remain the same, and the emissions in other East Asian countries continue to grow, for the worst case scenario in the year of 2020, the contribution from East Asia to the MADMO₃ concentration would increase by 3.7 ppb.

We also used the indicator equations proposed by Chen and Chang (2006) to evaluate the O₃ sensitivity of land grid cells in Taiwan. The simulation results of the Base case indicated that of the areas polluted by O₃ in Taiwan, the ratio of VSR is relatively high (72%). This suggests that controlling VOC emissions should be a priority for Taiwan in order to reduce high levels of O₃ pollution. The VSR ratio has dropped to 55% and the importance of NSR has increased in Case 2020. Also, the emission control strategies for O₃ improvement should be gradually adjusted and employed to equally emphasize the NO_x and VOCs reduction, instead of merely placing the emphasis on the reduction of VOCs in response to the possible growth of future emissions in East Asia, even though the VOC volume is still the priority in Taiwan.

Because the variations in wind fields across different seasons enable the polluted air masses of different degrees of aging emitted in East Asia to be transported into Taiwan. This further results in a different transition of O₃ sensitivity in various seasons in Taiwan, which is mainly attributed from an increase in LRT. In winter, pollutants are imported directly and rapidly into Taiwan. For this reason, the polluted air mass is relatively fresh, and the O₃ sensitivity of areas highly polluted with O₃ tend significantly toward VSR. In summer, spring, and fall, the pollutants are transported more slowly (lower wind velocity) or over longer distances (imported from high altitudes, or from oceans south of Taiwan); thus, the polluted air mass is relatively aged, and so the O₃ sensitivity of those areas highly polluted with O₃ would significantly tend toward NSR.

REFERENCES

- Berntsen, T., Isaksen, I.S., Wang, W.C., and Liang, X.Z. (1996). "Impacts of increased anthropogenic emissions in Asia on tropospheric ozone and climate: A global 3-D model study." *Tellus B: Chemical and Physical Meteorology*, **48**(1), 13-32.
- Blanchard, C.L., and Fairley, D. (2001). "Spatial mapping of VOC and NO_x-limitation of ozone formation in central California." *Atmospheric Environment*, **35**(22), 3861-3873.
- Chang, J.S., Middleton, P.B., Stockwell, W.R., Walcek, C.J., Pleim, J. E., Lansford, H. H., and Hass, H. (1990). "The regional acid deposition model and engineering model, acidic deposition: State of Science and Technology, Report 4." *National Acid Precipitation Assessment Program*.
- Chang, J.S., Brost, R.A., Isaksen, I.S.A., Madronich, S., Middleton, P., Stockwell, W.R., and Walcek, C.J. (1987). "A three-dimensional Eulerian acid deposition model: Physical concepts and formulation." *Journal of Geophysical Research: Atmospheres*, **92**(D12), 14681-14700.
- Chang, K.H., Yu, J.Y., Chen, T.F., and Lin, Y.P. (2009). "Estimating Taiwan biogenic VOC emission: Leaf energy balance consideration." *Atmospheric Environment*, **43**(32), 5092-5100.
- Chang, K.H., Jeng, F.T., Tsai, Y.L., and Lin, P.L. (2000). "Modeling of long-range transport on Taiwan's acid deposition under different weather conditions." *Atmospheric Environment*, **34**(20), 3281-3295.
- Chen, T.F. and Chang, K.H. (2006). "Formulating the relationship between ozone pollution features and the transition value of photochemical indicators." *Atmospheric Environment*, **40**(10), 1816-1827.
- Chen, T.F., Chen, C.H., Yu, J.Y., Lin, Y.B., and Chang, K.H. (2020). "Estimation of biogenic VOC emissions in East Asia with new emission factors and leaf energy balance considerations." *J. Innov. Technol.*, **2**(2), 61-72. doi.org/10.29424/JIT.202009_2(2).0010
- Chock, D.P., Chang, T.Y., Winkler, S.L., and Nance, B.I. (1999). "The impact of an 8 h ozone air quality standard on ROG and NO_x controls in Southern California." *Atmospheric Environment*, **33**(16), 2471-2485.
- Chou, C.C. K., Liu, S.C., Lin, C.Y., Shiu, C.J., and Chang, K.H. (2006). "The trend of surface ozone in Taipei, Taiwan, and its causes: Implications for ozone control strategies." *Atmospheric Environment*, **40**(21), 3898-3908.
- Emery, C., Tai, E., and Yarwood, G. (2001). "Enhanced meteorological modeling and performance evaluation for two Texas ozone episodes." *Prepared for the Texas natural resource conservation commission, by ENVIRON International Corporation*.
- Grell, G.A., Dudhia, J., and Stauffer, D.R. (1994). "A description of the fifth-generation Penn State/NCAR Mesoscale Model (MM5)." NCAR Technical Note, NCAR/TN-398+STR, Boulder, CO, 117pp.
- He, J., Zhang, Y., Wang, K., Chen, Y., Leung, L.R., Fan, J., and He, K. (2017). "Multi-year application of WRF-CAM5 over East Asia-Part I: Comprehensive evaluation and formation regimes of O₃ and PM_{2.5}." *Atmospheric Environment*, **165**, 122-142.
- Inoue, K., Tonokura, K., and Yamada, H. (2019). "Modeling study on the spatial variation of the sensitivity of photochemical ozone concentrations and population exposure to VOC emission reductions in Japan." *Air Quality, Atmosphere & Health*, **12**(9), 1035-1047.
- Jin, X., Fiore, A.M., Murray, L.T., Valin, L.C., Lamsal, L.N., Duncan, B., and Tonnesen, G.S. (2017). "Evaluating a space-based indicator of surface ozone-NO_x-VOC sensitivity over midlatitude source regions and application to decadal trends." *Journal of Geophysical Research: Atmospheres*, **122**(19), 10-439.
- Lu, C.H. and Chang, J.S. (1998). "On the indicator-based approach to assess ozone sensitivities and emissions features." *Journal of Geophysical Research: Atmospheres*, **103**(D3), 3453-3462.
- Nagashima, T., Ohara, T., Sudo, K., and Akimoto, H. (2010). "The relative importance of various source regions on East Asian surface ozone." *Atmospheric Chemistry and Physics*, **10**(22), 11305-11322.
- Ohara, T.A. H.K., Akimoto, H., Kurokawa, J.I., Horii, N., Yamaji, K., Yan, X., and Hayasaka, T. (2007). "An Asian emission inventory of anthropogenic emission sources for the period 1980-2020." *Atmospheric Chemistry and Physics*, **7**(16), 4419-4444.

- Richter, A., Burrows, J.P., Nüß, H., Granier, C., and Niemeier, U. (2005). "Increase in tropospheric nitrogen dioxide over China observed from space." *Nature*, **437**(7055), 129-132.
- Russell, A. and Dennis, R. (2000). "NARSTO critical review of photochemical models and modeling." *Atmospheric environment*, **34**(12-14), 2283-2324.
- Sillman, S. and He, D. (2002). "Some theoretical results concerning O₃-NO_x-VOC chemistry and NO_x-VOC indicators." *Journal of Geophysical Research: Atmospheres*, **107**(D22), ACH-26.
- Sillman, S., He, D., Cardelino, C., and Imhoff, R. E. (1997). "The use of photochemical indicators to evaluate ozone-NO_x-hydrocarbon sensitivity: Case studies from Atlanta, New York, and Los Angeles." *Journal of the Air & Waste Management Association*, **47**(10), 1030-1040.
- Taiwan EPA, 2009. "The Manual of Air Pollutants Emission Estimation in Taiwan." Final Report, China Technological Consultant Inc., Taipei, Taiwan (in Chinese).
- Tanimoto, H. (2009). "Increase in springtime tropospheric ozone at a mountainous site in Japan for the period 1998-2006." *Atmospheric Environment*, **43**(6), 1358-1363.
- Tonnesen, G.S. and Dennis, R.L. (2000). "Analysis of radical propagation efficiency to assess ozone sensitivity to hydrocarbons and NO_x: 1. Local indicators of instantaneous odd oxygen production sensitivity." *Journal of Geophysical Research: Atmospheres*, **105**(D7), 9213-9225.
- Wang, K. Y. (2005). "A 9-year climatology of airstreams in East Asia and implications for the transport of pollutants and downstream impacts." *Journal of Geophysical Research: Atmospheres*, **110**(D7).
- Wang, T., Wei, X.L., Ding, A.J., Poon, C.N., Lam, K.S., Li, Y.S., and Anson, M. (2009). "Increasing surface ozone concentrations in the background atmosphere of Southern China, 1994-2007." *Atmospheric Chemistry and Physics*, **9**(16), 6217-6227.
- Wolff, G.T., Liou, P.J., Wight, G.D., Meyers, R.E., and Cederwall, R.T. (1977). "An investigation of long-range transport of ozone across the midwestern and eastern United States." *Atmospheric Environment (1967)*, **11**(9), 797-802.
- Xu, X.B., Lin, W.L., Wang, T., Meng, Z., and Wang, Y. (2006). "Long-term trend of tropospheric ozone over the Yangtze Delta Region of China." *Advances in climate change research*, **2**(5), 211-216.

